

Supplementary Information

Controllable Porosity Conversion of Metal-Organic Frameworks Composed of Natural Ingredients for Drug Delivery

Jiang Liu,^{a,b†} Tian-Yi Bao,^{c†} Xi-Ya Yang,^a Pei-Pei Zhu,^a Lian-He Wu,^d Jing-Quan Sha,^{*a,d} Lei Zhang,^b Long-Zhang Dong,^b Xue-Li Cao,^b Ya-Qian Lan^{*b}

^aKey Laboratory of Inorganic Chemistry in Universities of Shandong, Department of Chemistry and Chemical Engineering, Jining University, Qufu, Shandong, 273155, China shajq2002@126.com

^bJiangsu Key Laboratory of Biofunctional Materials, College of Chemistry and Materials Science, Nanjing Normal University, Nanjing 210023, P. R. China. yqlan@nynu.edu.cn

^cThe Second Hospital of Jilin University, Changchun, 130041, P. R. China

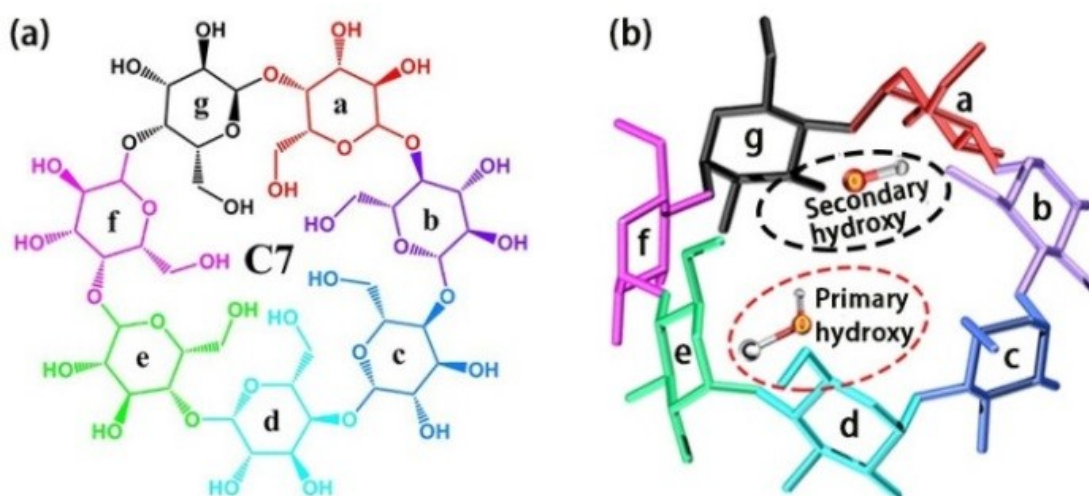
^dThe Provincial Key Laboratory of Biological Medicine Formulation, School of Pharmacy, Jiamusi University, Heilongjiang, Jiamusi, 154007, PR China

E-mail: shajq2002@126.com; yqlan@nynu.edu.cn

Contents

1. Additional figures.....	S2
2. Experimental and crystallographic details	S2
3. Template agent considerations	S4
4. Drug loading and release	S9
5. In vitro Cytotoxicity test	S14

1. Additional figures



Scheme S1 | Structural formula (a) and stereo drawing (b) of β -cyclodextrin (β -CD) composed of seven asymmetric (C1) α -1,4-linked D-glucopyranosyl residues, with C7-asymmetric arrangement, incorporating seven of the monosaccharide residues in the form of a torus with a diameter of 6.6 Å. The seven primary hydroxy ($-\text{CH}_2\text{OH}$) groups and the seven glycosidic ring oxygen atoms constitute the primary face of β -CD molecule, while the fourteen secondary hydroxy ($-\text{CHOH}$) groups constitute the secondary face.

2. Experimental and synthetic details

General methods and materials: All reagents were purchased commercially and used without further purification. Elemental analysis (C and H) is performed on a Perkin-Elmer 2400 CHN Elemental Analyzer. The IR spectra were obtained on an Alpha Centaur FT/IR spectrometer with KBr pallet in the 400-4000 cm^{-1} region. XRPD patterns were obtained with a Rigaku D/max 2500V PC diffractometer with Cu-K α radiation, the scanning rate is 4°/s, 2 θ ranging from 5-40°. UV-vis absorption spectra were recorded on a 756 CRT UV-vis spectrophotometer.

Synthesis of $\text{Cs}(\text{OH})\cdot(\text{C}_{42}\text{H}_{70}\text{O}_{35})$ (CD-MOF-1): β -Cyclodextrin (1.1g, 1 mmol), CsCl (0.3 g, 2 mmol) and H_3tzdc (0.1, 0.6 mmol) were dissolved with CH_3OH (10 ml), the resulting solution was stirred for 30 min at room temperature, and then transferred into a Teflon-lined stainless steel autoclave (20 ml). The Teflon-lined stainless steel autoclave was kept at 160°C for 3 days followed by cooling to room temperature at a rate of 5 °C/h. Colorless block crystals were obtained. The products were washed with analytically pure MeOH for three times and then collected by filtration. Elemental analysis calcd (%) for $\text{CsC}_{42}\text{H}_{71}\text{O}_{36}$ (1284.9): C 39.22, H 5.52; found: C 39.19; H 5.62.

Synthesis of $[\text{Cs}_{1.5}(\text{C}_{42}\text{H}_{66.5}\text{O}_{35})]_2$ (CD-MOF-2): β -Cyclodextrin (1.1g, 1 mmol), CsCl (0.3 g, 2 mmol) and TsOH (0.1 g, 0.6 mmol) were dissolved with CH_3OH (10 ml), the resulting solution was stirred for 30 min at room temperature, and then transferred into a Teflon-lined stainless steel autoclave (20 ml). The Teflon-lined stainless steel autoclave was kept at 160°C for 4 days followed by cooling to room temperature at a rate of 5 °C/h. Colorless block crystals were filtered. The products were washed with analytically pure MeOH for three times and collected by filtration. Elemental analysis calcd (%) for $\text{Cs}_3\text{C}_{84}\text{H}_{133}\text{O}_{70}$ (2661.63): C 37.87, H 4.99; found: C 37.98; H 5.14.

Crystallographic data collections and refinement: Structural measurements for CD-MOF-1 and CD-MOF-2 were performed on a Rigaku RAXIS RAPID IP diffractometer with Mo-K α monochromatic radiation ($\lambda = 0.71069$ Å) at 293 K. The structures were solved by the directed methods and refined by full matrix least-squares on F² using the SHELXL and OLEX2 crystallographic software packages.¹ All non-hydrogen atoms in CD-MOF-1 and CD-MOF-2 were refined anisotropically. The positions of hydrogen atoms on carbon atoms were calculated theoretically. Attempts to locate and model the solvent molecules in the pores were unsuccessful. Therefore, we employed PLATON/SQUEEZE2 to calculate the contribution to diffraction from the solvent region and thereby produced a set of solvent-free diffraction intensities. The crystal data for CD-MOF-1 and CD-MOF-2 are summarized in Table S1. Since the metrical parameters associated with these structures are unexceptional, some of bond lengths relative to the M sites are given in Table S4. Crystallographic data for the structure reported in this paper have been deposited in the Cambridge Crystallographic Data Center with CCDC Number 1404895 for CD-MOF-1 and 1407798 for CD-MOF-2.

Table S1 | Selected Crystallographic Data for CD-MOFs.

Compound	CD-MOF-1	CD-MOF-2
Chemical formula	CsC ₄₂ H ₇₁ O ₃₆	Cs ₃ C ₈₄ H ₁₃₃ O ₇₀
Formula weight	1284.9	2661.63
Temperature (K)	293(2)	293(2)
Wavelength (Å)	0.71069	0.71069
Crystal system	Monoclinic	Monoclinic
Space group	<i>P</i> 2 ₁	<i>C</i> 2
<i>a</i> (Å)	15.026(5)	21.981(5)
<i>b</i> (Å)	15.265(3)	25.367(5)
<i>c</i> (Å)	15.120(6)	15.790(5)
α (°)	90.00	90.00
β (°)	119.19	133.55
γ (°)	90.00	90.00
<i>V</i> (Å ³) / <i>Z</i>	3027.6 / 2	6381 / 2
Density (g·cm ⁻³)	1.403	1.385
Abs coeff. (mm ⁻¹)	0.705	0.949
<i>F</i> (000)	1320	2724.0
Data collect ϑ range	3.78-25.00°	3.69- 26.81
Reflns collected	12104	17898
Independent reflns	7894	9384
<i>R</i> _{int}	0.0257	0.0269
Refinement method on <i>F</i> ²	Full-matrix least-squares	Full-matrix least-squares
Data/restraints/parameters	7894/1/707	9384/10/740
Goodness-of-fit on <i>F</i> ²	1.087	1.032
Final <i>R</i> indices [<i>I</i> > 2 σ (<i>I</i>)]	<i>R</i> ₁ = 0.0838, <i>wR</i> ₂ = 0.2372	<i>R</i> ₁ =0.0543, <i>wR</i> ₂ = 0.1450
<i>R</i> indices (all data)	<i>R</i> ₁ = 0.0975, <i>wR</i> ₂ = 0.2534	<i>R</i> ₁ =0.0607, <i>wR</i> ₂ = 0.1509
$R_1 = \sum (F_o - F_c) / \sum F_o $, $wR_2 = \sum w(F_o ^2 - F_c ^2)^2 / \sum w(F_o ^2)^2]^{1/2}$		

3. Template agent considerations:

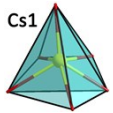
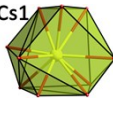

This is not to deny that the serendipity usually bundled with hydrothermal/solvothermal method exerts its efficiency to the successful construction of targeted CD-MOFs, while a certain degree of “design” is indeed present in our choice of template agents, which expected to alter the packing fashion of β -CD molecules during the self-assembly process via supramolecular interaction. To further evidence the validity of this strategy, a great deal of parallel experiments concerning other possible influential factors, such as solvent, temperature, the ratio of metal salt to β -CD molecules and hydrothermal/solvothermal method, were carried out to strengthen the contrast so as to make the eventual conclusion deduced more reasonable. Ultimately, a series of important findings extracted from our control experiments (Table S2) are shown as follows: (i) CD-MOF-1 can be obtained no matter there is short template molecule ($H_3tzdc < 5\text{\AA}$) or not, but its poor crystallinity seems to be enhanced only in the case of template molecule. (ii) The formation of CD-MOF-2 has to be triggered by adding long template molecule ($TsOH/IBU > 6\text{\AA}$). (iii) Amorphous product or powder occurs when the reaction proceeds under the condition of hydrothermal synthesis. As we can see from these facts, different template molecule (H_3tzdc , $TsOH$ or IBU) appeared in the reaction process really is a pivotal component to affect the porosity and crystallization of resultant CD-MOF. Meanwhile, the decreased volume of H_2O within mixed solvent (H_2O and $MeOH$) was proved to be more beneficial for the crystallization of CD-MOFs, which is different from the fact that the mixed solvent is always a favourable condition for synthesizing γ -CDs reported in some significant works. Although our control experiments could not used to interpret the most accurate role played by template molecules, we still hope to propose a seemingly available tactic to give some enlightenment for the construction of more CD-MOFs.

In the course of synthesizing the targeted CD-MOFs, we found that the 2D layer structure of CD-MOF-1 can easily obtained. Given that the stability of the overall framework, the adjacent 2D layers were stacked asymmetrically by supramolecular interaction that make the primary face and secondary face of each β -CD molecule to be occupied by other β -CD molecules, and then results in distinct “gourd-shaped” channels. To alter this type of “malposition” stacking fashion and obtain novel porous structure, we attempt to use specific organic molecule as template agent to guide the packing effect of β -CD molecules during the reaction process by means of supramolecular interaction or non-covalent interaction. As is well known to all, the nature of template molecules commonly needs to meet some requirements including size, shape, charge, etc. On this foundation, the short H_3tzdc (ca. $4.6\text{\AA} \times 4.5\text{\AA}$) was selected firstly as template molecule that not only can entirely accommodate itself into the β -CD (ca. $5.2\text{\AA} \times 6.6\text{\AA}$) molecule but also facilitates the robustness of β -CD molecules that is conducive to the crystallization of compound, by introducing inclusion complexation and non-covalent interaction. Whereas these intramolecular interactions are too weak to further influence the surrounding β -CD molecules, it is unable to dominate the formation of new cavity characteristics, except improving the crystallinity of CD-MOF-1. When the sizes of selected template molecules (ca. $6.8\text{\AA} \times 3.8\text{\AA}$ for $TsOH$ and ca. $9.2\text{\AA} \times 5.2\text{\AA}$ for IBU drug) are comparable to that of β -CD, CD-MOF-2 with uniformly 1D channels was isolated, since the terminal moieties of templates are easily interacting with other outside β -CD molecules to form intermolecular interactions that finally interferes the arrangement of β -CD molecules within the crystal lattice. In this sense, we are inclined to believe the proper length of organic ligands is the underlying reason for the formation of targeted structures with different porosity. This result also indicates that the long template molecule can avoid the formation of networks involved in interpenetration, interweaving, or staggered arrangement. More importantly, these template molecules does not crystallize within the resultant CD-MOFs would endow the host frameworks with well loading capacities that can used for drug delivery applications.

Table S2 | Influences of the template molecules employed, the ratio of metal to β -CD, solvent and temperature to the preparation of targeted CD-MOFs.

Complex	Template molecules	CsCl: β -CD/ β -CD:CsCl	H ₂ O:MeOH	Temperature (°C)	Product morphology Powder/Crystal (Poor/Good)
CD-MOF-1	No	1:1/1:2/1:5	10:0/8:2/5:5/2:8/0:10	120	Powder/Crystal (Poor/Good)
CD-MOF-1	No	1:1/1:2/1:5	10:0/8:2/5:5/2:8/0:10	140	Powder/Crystal (Poor/Good)
CD-MOF-1	No	1:1/1:2/1:5	10:0/8:2/5:5/2:8/0:10	160	Powder/Crystal (Poor/Good)
CD-MOF-1	H ₃ tzdc	1:1/1:2/1:5	10:0/8:2/5:5/2:8/0:10	120	Powder/Crystal (Good)
CD-MOF-1	H ₃ tzdc	1:1/1:2/1:5	10:0/8:2/5:5/2:8/0:10	140	Powder/Crystal (Good)
CD-MOF-1	H ₃ tzdc	1:1/1:2/1:5	10:0/8:2/5:5/2:8/0:10	160	Powder/Crystal (Good)
CD-MOF-2	TsOH	1:1/1:2/1:5	10:0/8:2/5:5/2:8/0:10	120	Powder/Crystal (Poor/Good)
CD-MOF-2	TsOH	1:1/1:2/1:5	10:0/8:2/5:5/2:8/0:10	140	Powder/Crystal (Poor/Good)
CD-MOF-2	TsOH	1:1/1:2/1:5	10:0/8:2/5:5/2:8/0:10	160	Powder/Crystal (Poor/Good)
CD-MOF-2	IBU	1:1/1:2/1:5	10:0/8:2/5:5/2:8/0:10	120	Powder/Crystal (Poor/Good)
CD-MOF-2	IBU	1:1/1:2/1:5	10:0/8:2/5:5/2:8/0:10	140	Powder/Crystal (Poor/Good)
CD-MOF-2	IBU	1:1/1:2/1:5	10:0/8:2/5:5/2:8/0:10	160	Powder/Crystal (Poor/Good)

Table S3 | Cesium ions geometry analysis of CD-MOFs by using Continuous Shape Measurements (CShM).^a

	HP-6 (D _{6h})	PPY-6 (C _{5v})	OC-6 (O _h)	TPR-6 (D _{3h})	JPPY-5 (C _{5v})		
CD-MOF-1	23.42	9.36	26.19	17.45	13.88		
	PPR-10 (D _{5h})	PAPR-10 (D _{5d})	JBCCU-10 (D _{4h})	JMBIC-10 (C _{2v})	SDD-10 (D ₂)	TD-10 (C _{2v})	HD-10 (D _{4h})
CD-MOF-2	6.58	7.03	12.05	10.09	5.19	7.22	9.80
	PPR-10 (D _{5h})	PAPR-10 (D _{5d})	JMBIC-10 (C _{2v})	JSPC-10 (C _{2v})	SDD-10 (D ₂)	TD-10 (C _{2v})	HD-10 (D _{4h})
CD-MOF-2	10.86	9.97	9.22	7.70	7.26	8.63	8.43
<p>HP-6 = Hexagon; PPY-6 = Pentagonal pyramid; OC-6 = Octahedron; TPR-6 = Trigonal prism; JPPY-5 = Johnson pentagonal pyramid (J2); PPR-10 = Pentagonal prism; PAPR-10 = Pentagonal antiprism; JBCCU-10 = Bicapped cube (Elongated square bipyramid J15); JMBIC-10 = Metabidiminshed icosahedron (J62); JSPC-10 = Sphenocorona (J87); SDD-10 = Staggered dodecahedron (2:6:2); TD-10 = Tetradecehedron (2:6:2); HD-10 = Hexadecahedron (2:6:2, or 1:4:4:1). ^a (a) Alvarez, S., Alemany, P., Casanova, D., Cirera, Lluell, J., M., Avnir, D. <i>Coord. Chem. Rev.</i>, 2005, 249, 1693-1708; (b) Casanova, D., Lluell, M., Alemany, P., Alvarez, S. <i>Chem. Eur. J.</i>, 2005, 11, 1479-1494.</p>							

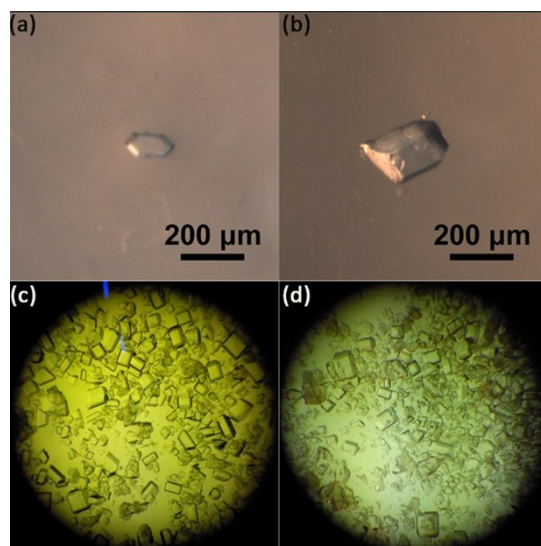


Figure S1 | The sizes and morphologies of (a, c) CD-MOF-1 and (b, d) CD-MOF-2.

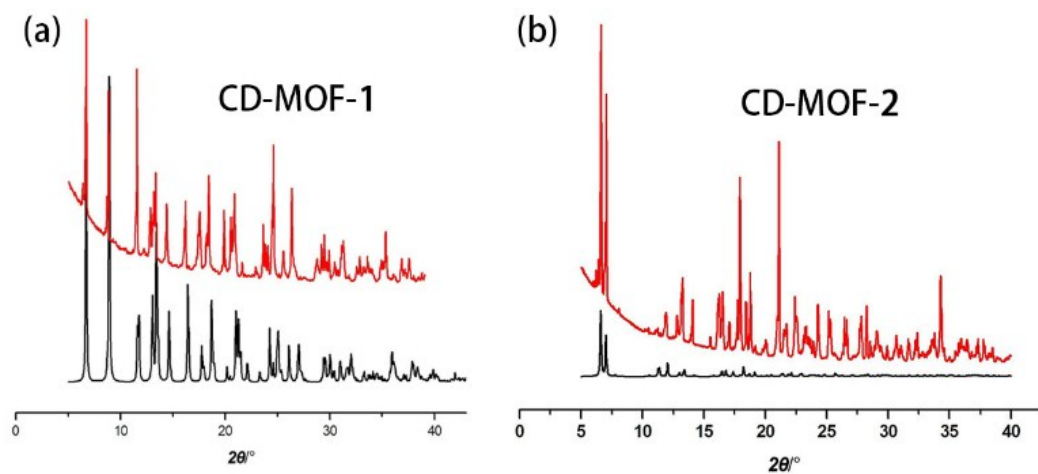


Figure S2 | PXRD patterns for the simulated (black) and as-synthesized (red) samples (a, CD-MOF-1; b, CD-MOF-2)

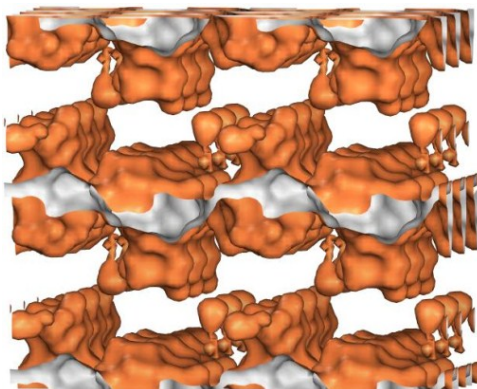


Figure S3 | Accessible voids of CD-MOF-1 viewed along crystallographic a axis.

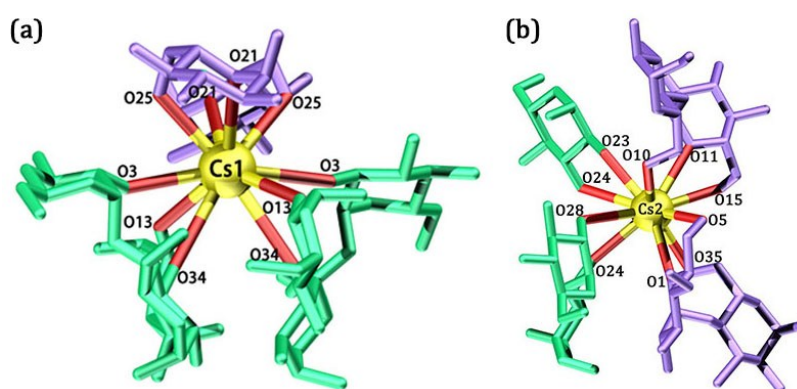


Figure S4 | Coordination spheres of Cs1 (a) and Cs2 (b) ions in CD-MOF-2.

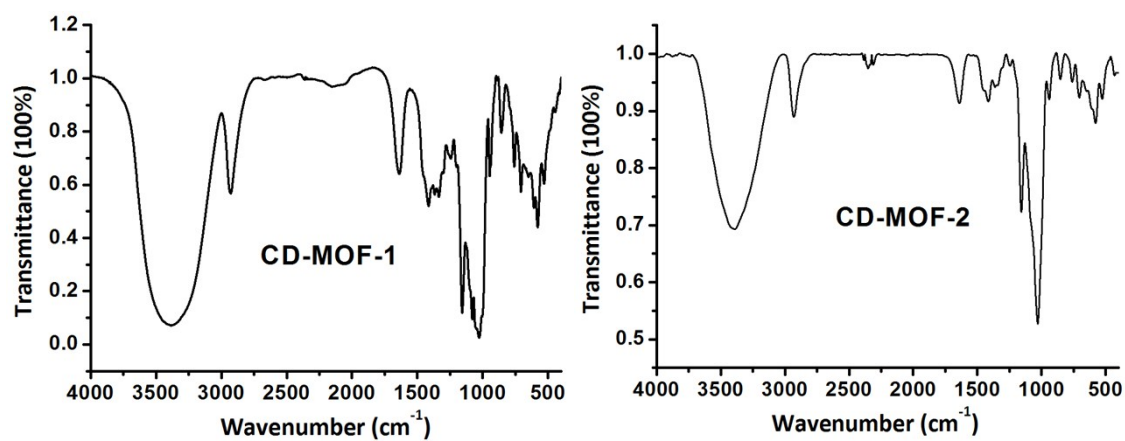


Figure S5 | The IR spectra of CD-MOF-1 (*left*) and CD-MOF-2 (*right*).

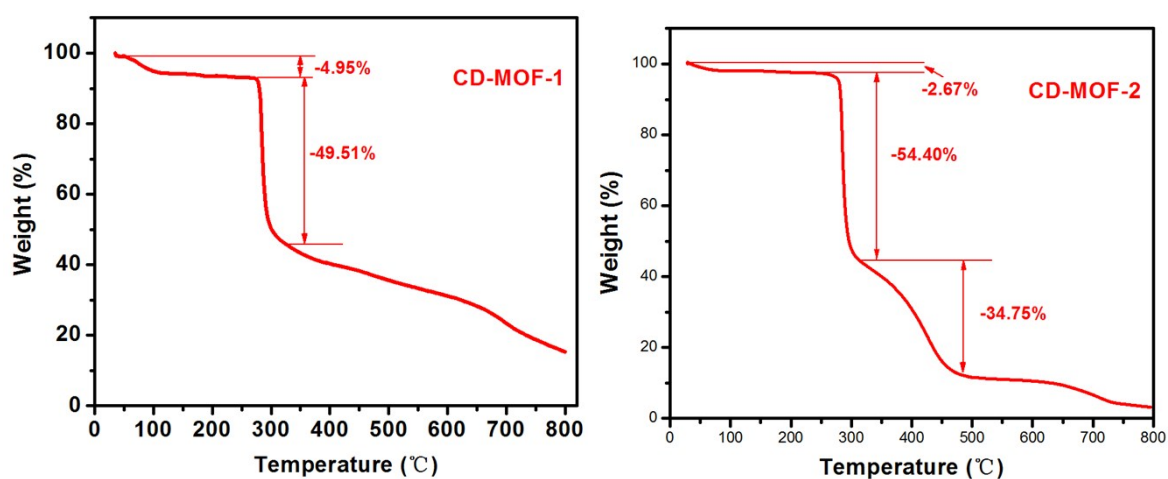


Figure S6. Thermogravimetric analysis for CD-MOF-1 and CD-MOF-2 under N₂ (*red*) atmosphere (10 K min⁻¹).

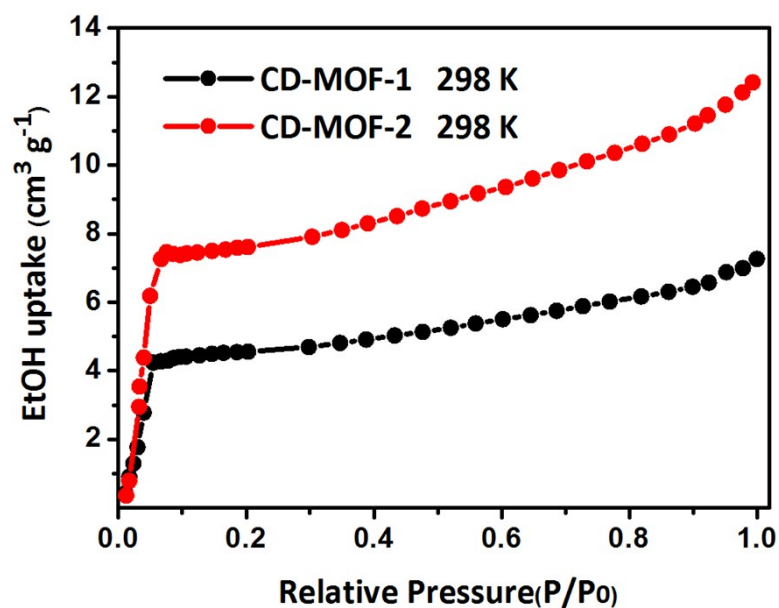


Figure S7. Ethanol-vapor-adsorption isotherms for activated CD-MOFs at 298 K.

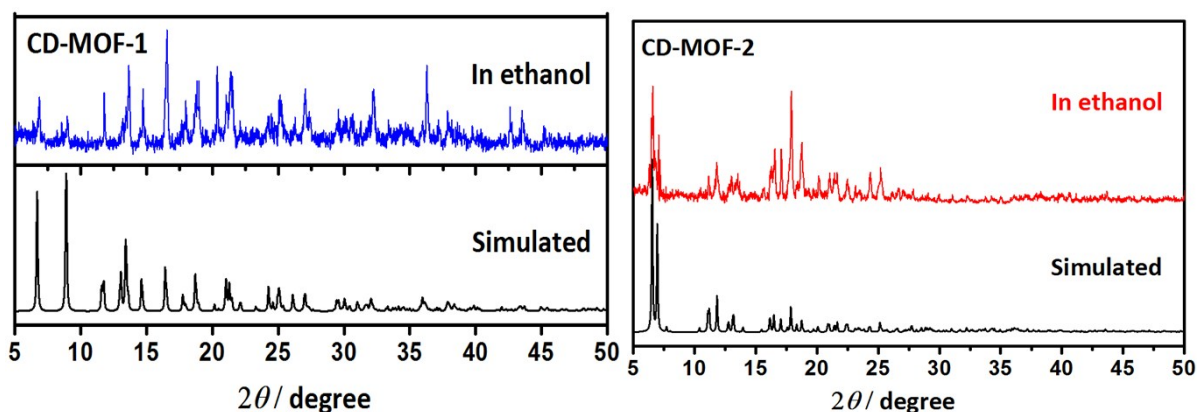


Figure S8 | (left) PXRD patterns for CD-MOF-1 (simulated, black; sample immersed in ethanol for six days, blue) and (right) CD-MOF-2 (simulated, black; sample immersed in ethanol for six days, red).

Table S4 | Bond lengths (Å) around Cs ions in the crystal structures of CD-MOF-1 and CD-MOF-2.

Compound	M ⁺	M ⁺ -Primary OH	M ⁺ -ring O	M ⁺ -Secondary OH	M ⁺ -Secondary OH
CD-MOF-1	Cs1	3.101 (Cs-O15) 3.079 (Cs-O30)	3.285 (Cs-O1) 3.486 (Cs-O12)	3.056 (Cs-O8)	3.148 (Cs-O9)
CD-MOF-2	Cs1	3.197(Cs-O25)	3.572(Cs-O21)	3.263(Cs-O3) 3.337(Cs-O13)	3.609(Cs-O34)
CD-MOF-2	Cs2	3.082(Cs-O5) 3.414(Cs-O10) 3.539(Cs-O15) 3.445(Cs-O35)	3.116(Cs-O11) 3.541(Cs-O1)	3.071(Cs-O23)	3.283(Cs-O24) 3.388(Cs-O28)

4. Drug Loading and Release

Immersing activated CD-MOF-1 / CD-MOF-2 (25 mg) sample into the 5-Fluorouracil (5-FU) / methotrexate (MTX) (75mg) dissolved ethanol (25 mL) solution for six days yielded heterogeneous solution. The mixture was centrifuged and then the solid was washed with ethanol many times. The corresponding 5-FU/MTX content was finally calculated through UV/Vis spectrophotometry results ($\lambda = 264$ nm for 5-Fu; 266 nm for MTX). For releasing experiment, drug-loaded CD-MOF-1 / CD-MOF-2 of 20 mg was dissolved into 500mL of PBS buffer solution (pH = 7.4), and loaded into a dialysis bag, which was dialyzed against 3 mL of deionized water at 37°C. During each time interval, ca.1 mL of the solution was pulled out to test, and then decanted back when the test was over. The content of 5-FU/ MTX in the samples taken out was monitored by UV/Vis spectrophotometry, in which the detection wavelengths were 266 nm for 5-Fu and 272 nm for MTX, respectively.

The calibration curve equation

The precision amount of 5-FU was dissolved in phosphate buffer solution (pH=7.4), then making into a certain mass concentration as the reference substance solution: 3.6 $\mu\text{g}\cdot\text{ml}^{-1}$ (A), 5.4 $\mu\text{g}\cdot\text{ml}^{-1}$ (B), 7.2 $\mu\text{g}\cdot\text{ml}^{-1}$ (C), 9.0 $\mu\text{g}\cdot\text{ml}^{-1}$ (D), 10.8 $\mu\text{g}\cdot\text{ml}^{-1}$ (E), 12.6 $\mu\text{g}\cdot\text{ml}^{-1}$ (F), 14.4 $\mu\text{g}\cdot\text{ml}^{-1}$ (G), 16.2 $\mu\text{g}\cdot\text{ml}^{-1}$ (H). According to the UV spectrophotometer of 5-FU, the measure wavelength is determined to be 264 nm. The process of calibration curve equation is as follows:

$$Y_{5\text{-FU PBS}} = 0.0496x + 0.0182 \quad R^2 = 0.9997$$

According to the same method, the calibration curve equation of MTX in PBS were determined with 266nm, 5-FU and MTX in ethanol are as follows:

$$Y_{\text{MTX PBS}} = 0.0317x + 0.0065 \quad R^2 = 0.9999$$

$$Y_{5\text{-FU ethanol}} = 0.0533x + 0.004 \quad R^2 = 0.9991$$

$$Y_{\text{MTX ethanol}} = 0.0351x - 0.0131 \quad R^2 = 0.9971$$

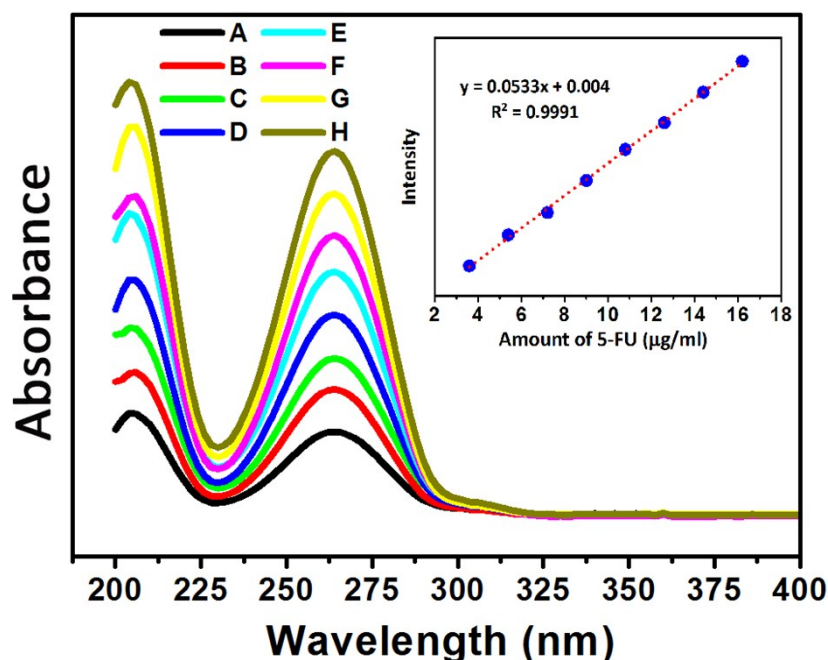


Figure S9 | The UV-vis absorption spectra and calibration curve (inset) of 5-FU in ethanol.

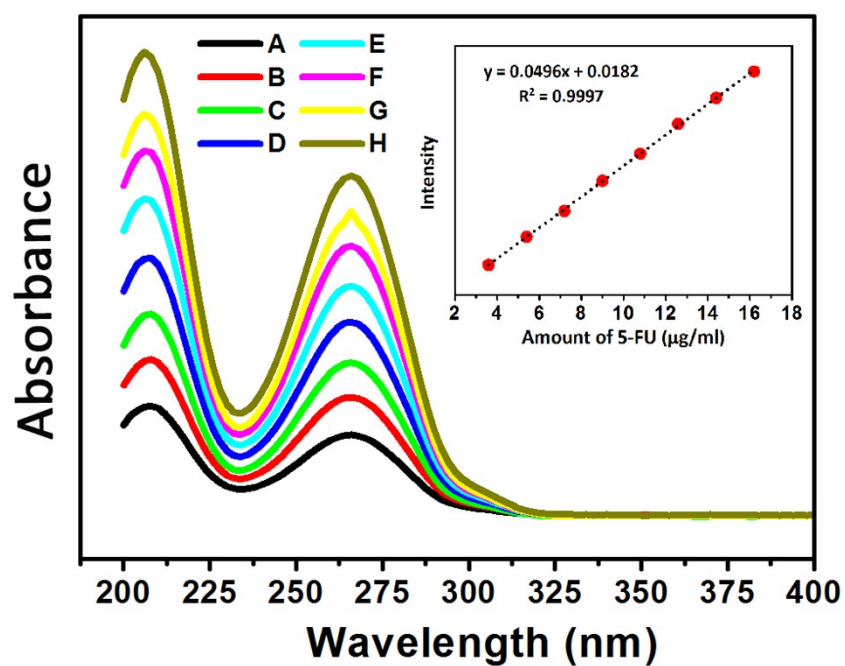


Figure S10 | The UV-vis absorption spectra and calibration curve (inset) of 5-FU in PBS buffer solution.

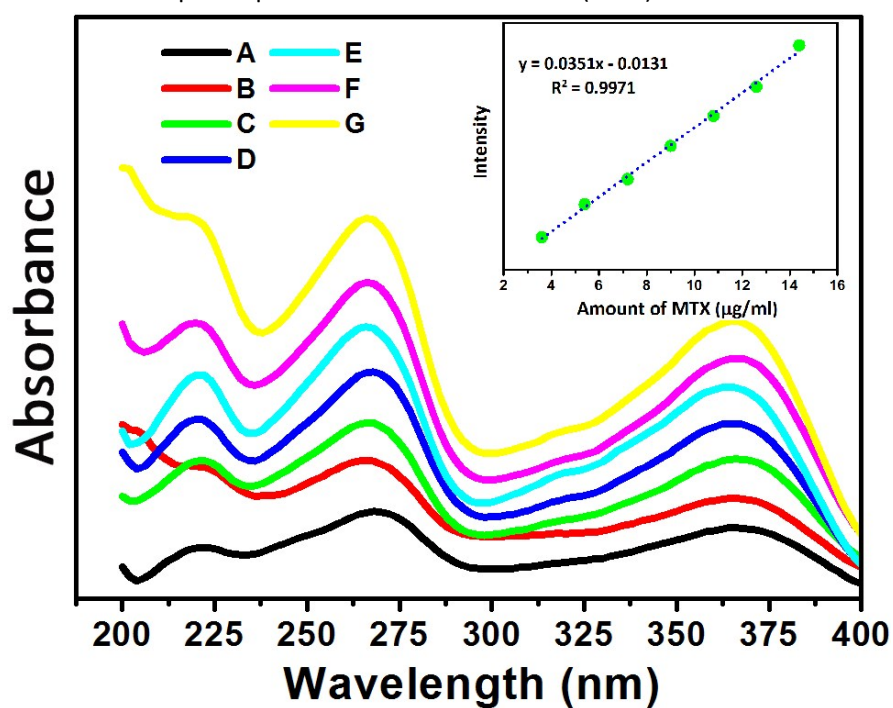


Figure S11 | The UV-vis absorption spectra and calibration curve (inset) of MTX in ethanol.

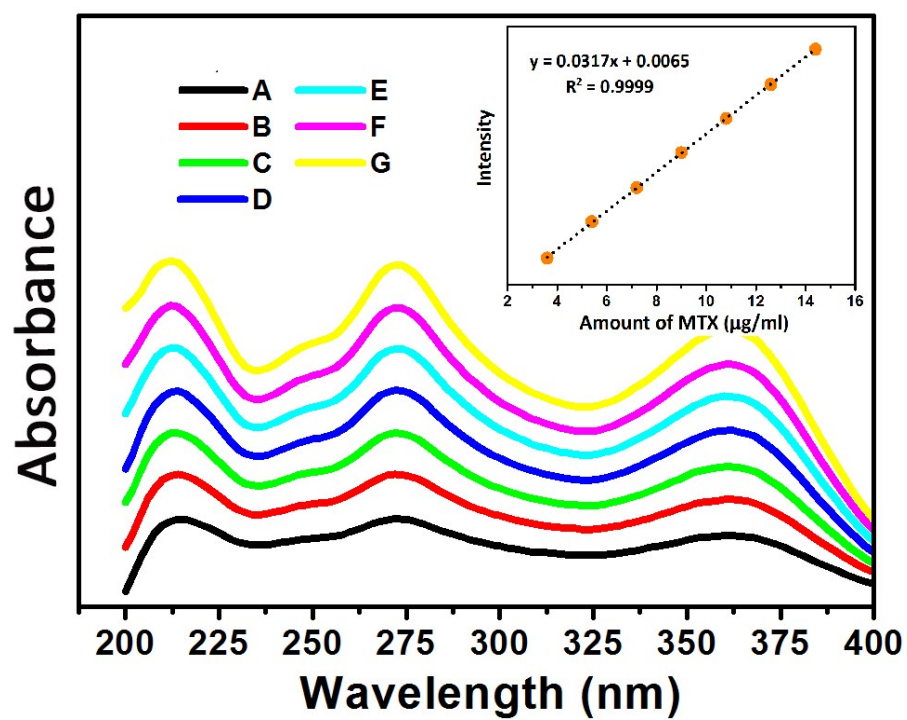


Figure S12 | The UV-vis absorption spectra and calibration curve (inset) of MTX in PBS buffer solution.

Drug Loading and Release:

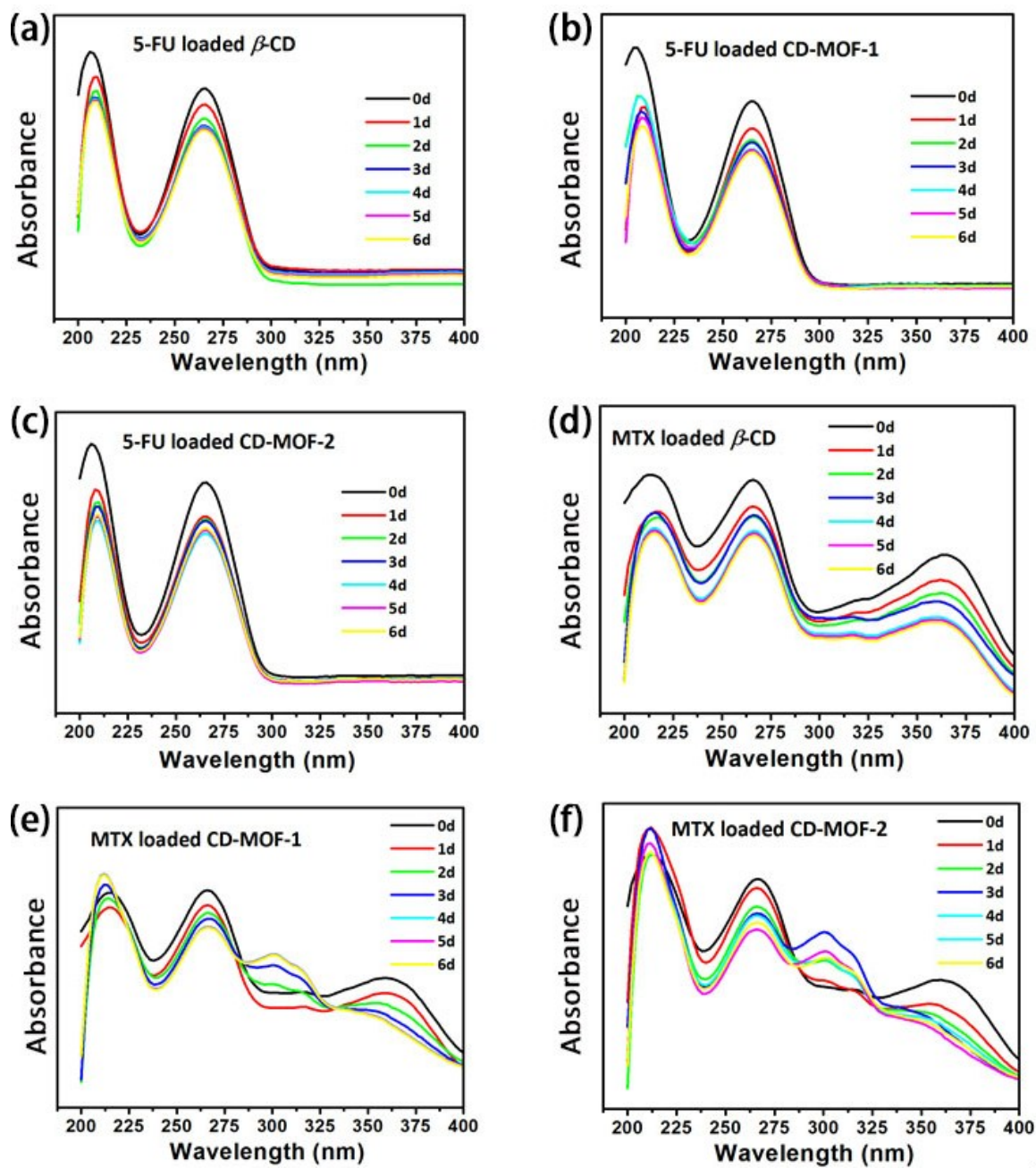


Figure S13 | The UV-Vis absorption spectra of 5-FU/MTX drug molecules loaded within β -CD (a, d), CD-MOF-1 (b, e) and CD-MOF-2 (c, f) during six days in ethanol.

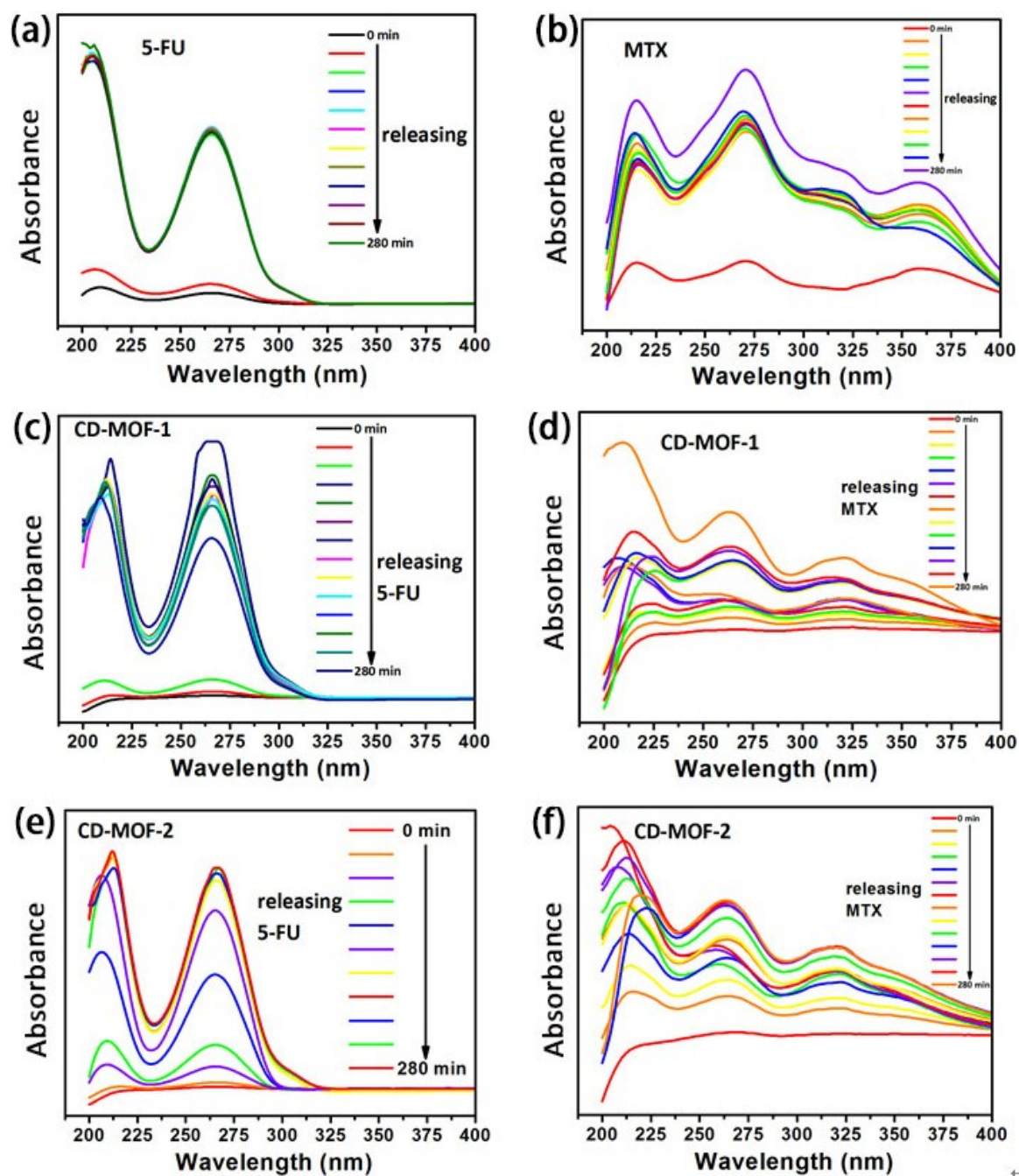


Figure S14 | The UV–Vis absorption spectra of 5-FU/MTX drug molecules releasing from themselves (a, b), CD-MOF-1 (c, d) and CD-MOF-2 (e, f) within 5h in PBS buffer solution.

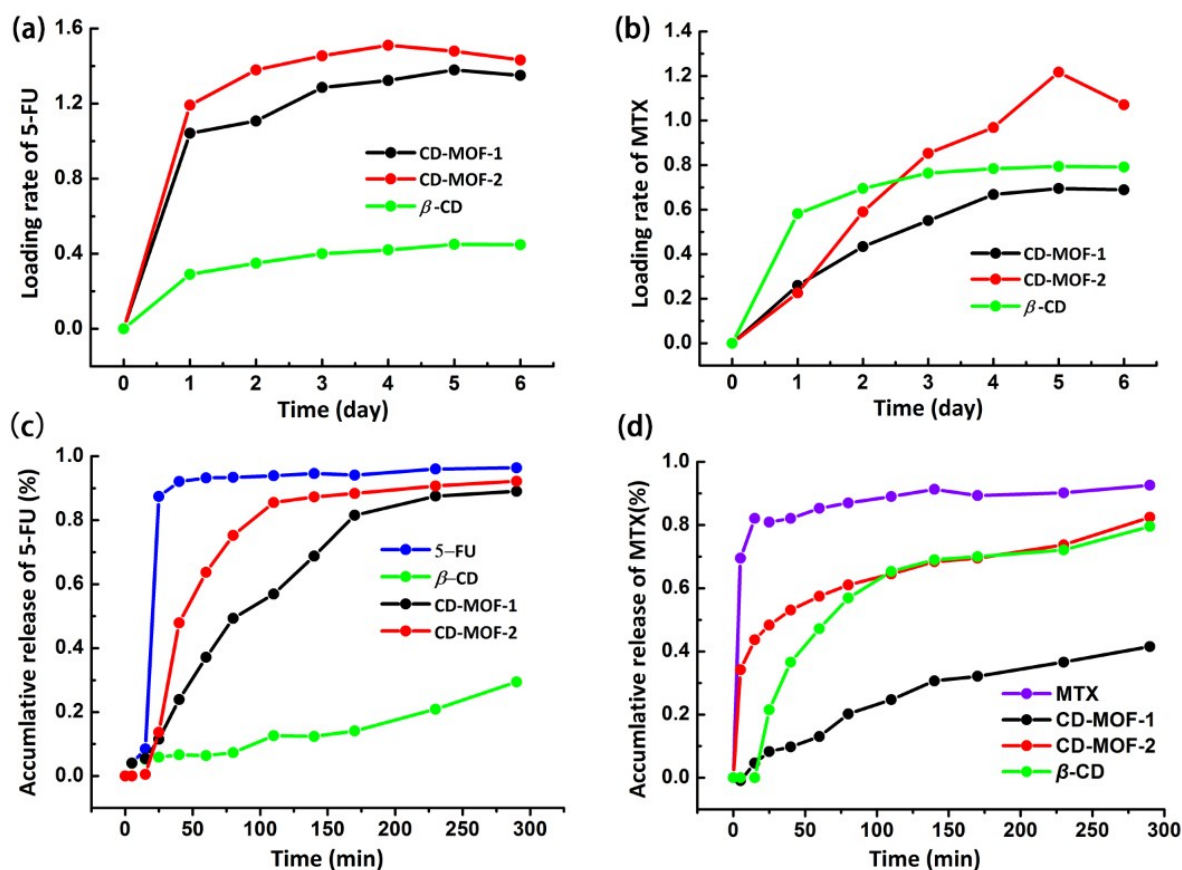


Figure S15 | Loading contents of 5-FU (a) and MTX (b) drug molecules to β -CD, CD-MOF-1 and CD-MOF-2. Release profiles of 5-FU (c) and MTX (d) drug molecules from targeted CD-MOFs under simulated biological conditions (PBS, pH = 7.4, 37°C).

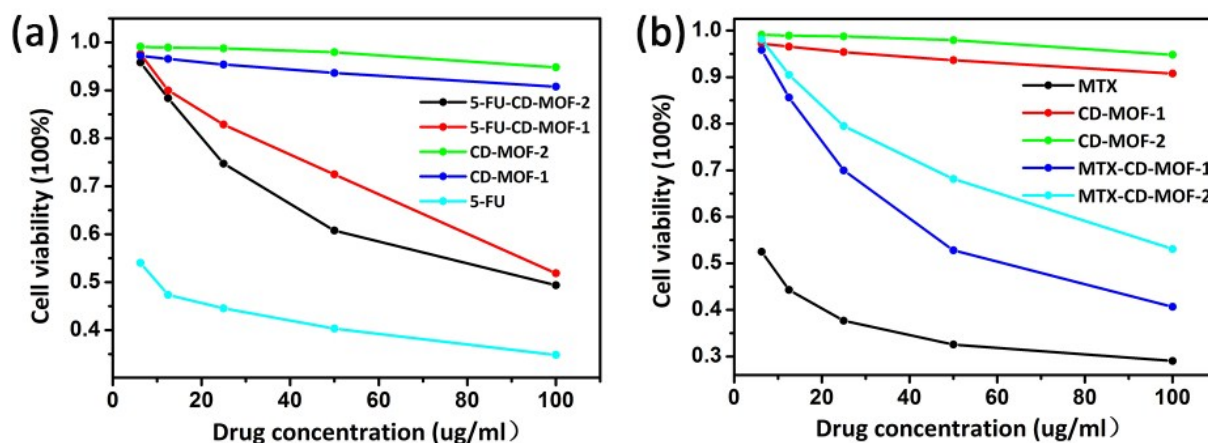


Figure S16 | Cytotoxicity tests on different drug (5-FU, a; MTX, b) loaded CD-MOFs against the HepG2 cells.

5. In vitro cytotoxicity assay

Human hepatoblastoma (HepG2) cells used in current study were routinely maintained in RPMI-1640 (GIBCO BRL), supplemented with 10% (v/v) heat-inactivated fetal calf serum (FCS), penicillin (100 U/mL), and streptomycin (100 μ g/mL) at 37°C under the condition of saturated humidity containing 5% CO₂ atmosphere. Cells were maintained in logarithmic phase with viability > 96%. HepG2 cells at a density of 105 per ml in a volume of 100 μ l per well were placed in 96-multiwell plates and incubated for 24 h.

The cytotoxicity study of compounds on HepG2 cells was tested by the Cell Counting Kit-8 (CCK-8) experiment. The experiments were divided into five groups, that is, blank control group (without HepG2 cells), negative control group (HepG2 cells without drug molecules), 5-FU drug group (HepG2 cells and drug molecules), CD-MOFs group (CD-MOF-1 and CD-MOF-2), 5-FU loaded group (5-FU-CD-MOF-1 and 5-FU-CD-MOF-2). The cells were incubated with every group at concentrations of 100, 50, 25, 12.5 and 6.25 $\mu\text{g}\cdot\text{ml}^{-1}$ for 24 h. Finally, CCK-8 (each hole with 10 μL) was added, the optical density (OD) values stemmed from the monitoring of BIV-TEK INSTRUMENTS INC at 540 nm. The corresponding cellular survival rate is determined with following equations:

$$\text{Survival rate (\%)} = (\text{OD}_{\text{compound}} - \text{OD}_{\text{blank}}) / (\text{OD}_{\text{negative}} - \text{OD}_{\text{blank}}) * 100\% \quad (1)$$

$$\text{Inhibitory rate (\%)} = 1 - \text{Survival rate (\%)} \quad (2)$$

According to the same method, another cytotoxicity investigation involving MTX drug molecules were also divided into similar five groups, that is, blank control group (without HepG2 cells), negative control group (HepG2 cells without drug molecules), MTX drug group (HepG2 cells and drug molecules), CD-MOFs group (CD-MOF-1 and CD-MOF-2), MTX loaded group (MTX-CD-MOF-1 and MTX-CD-MOF-2). The corresponding cellular survival rate can be obtained as above mentioned.

Table S5 | Optical density (OD) values observed in vitro cytotoxicity experiment for 5-FU, CD-MOF-1, CD-MOF-2, 5-FU-CD-MOF-1 and 5-FU-CD-MOF-2.

Compounds	6.25 $\mu\text{g}/\text{ml}$	12.5 $\mu\text{g}/\text{ml}$	25 $\mu\text{g}/\text{ml}$	50 $\mu\text{g}/\text{ml}$	100 $\mu\text{g}/\text{ml}$	Negative control	Blank control
5-FU	2.14	1.919	1.826	1.686	1.504	3.665	0.348
CD-MOF-1	3.913	3.889	3.846	3.782	3.678	4.015	0.365
CD-MOF-2	3.838	3.832	3.826	3.798	3.687	3.87	0.364
5-FU-CD-MOF-1	3.592	3.341	3.104	2.759	2.075	3.673	0.353
5-FU-CD-MOF-2	3.537	3.287	2.832	2.365	1.984	3.677	0.333

Table S6 | Optical density (OD) values observed in vitro cytotoxicity experiment for MTX, CD-MOF-1, CD-MOF-2, MTX-CD-MOF-1 and MTX-CD-MOF-2.

Compounds	6.25 $\mu\text{g}/\text{ml}$	12.5 $\mu\text{g}/\text{ml}$	25 $\mu\text{g}/\text{ml}$	50 $\mu\text{g}/\text{ml}$	100 $\mu\text{g}/\text{ml}$	Negative control	Blank control
MTX	2.212	1.923	1.6897	1.511	1.387	3.882	0.366
CD-MOF-1	3.913	3.889	3.846	3.782	3.678	4.015	0.365
CD-MOF-2	3.838	3.832	3.826	3.798	3.687	3.87	0.364
MTX-CD-MOF-1	3.763	3.401	2.845	2.234	1.803	3.912	0.358
MTX-CD-MOF-2	3.822	3.556	3.167	2.768	2.238	3.89	0.369

Table S7 | The 50% lethal concentration (IC_{50}) values against HepG2 cells calculated from the data of cytotoxicity assays.

Compounds	IC_{50} (ug/mL)	Compounds	IC_{50} (ug/mL)
5-FU	0.025	MTX	0.088
5-FU-CD-MOF-1	0.198	MTX-CD-MOF-1	0.178
5-FU-CD-MOF-2	0.187	MTX-CD-MOF-2	0.208